

Fig. 5 Aeroelastic responses of the first mode for a typical fighter wing with and without, control surface at  $M=0.825$ ,  $0.875$ , and  $0.925$ .

will have direct influence on the effectiveness of the active control surface. This phenomenon is demonstrated for a typical fighter wing.

The modes and frequencies of a typical fighter wing are given in Fig. 4. Based on the modal data, aeroelastic response analyses were conducted at the subsonic Mach number of  $0.825$ , and the transonic Mach numbers of  $0.850$ ,  $0.875$ ,  $0.900$ , and  $0.925$  for wings with and without control surface. For these cases, a control law that is effective in the lower transonic regime was used. The active control law selected corresponds to  $G_1 = -0.0002$ ,  $L_1 = \dot{q}_1$ , and  $\psi_1 = 0.0$  of Eq. (1). The first modal generalized velocity  $\dot{q}_1$  is obtained from solving Eq. (2) by numerical integration.<sup>5</sup> The results from these analyses showed that the control surface with the given control law was effective in the subsonic regime and slightly more effective in the transonic regime when the shock was forward of the control surface hinge line. The first modal responses of the fighter wing cases for the subsonic Mach number of  $0.825$  and the transonic Mach numbers of  $0.875$  and  $0.925$  are shown in Fig. 5. Higher modes were observed to play less significant roles in the overall response and were relatively unaffected by the active controls. By observing the damping rate of the first modal responses, it is noted that the control law remains effective in both the subsonic and transonic regimen up until the shock location has moved aft of the control surface hinge line. At  $M=0.925$ , when the shock has moved aft of the control surface hinge line, the control law becomes significantly less

effective. This trend was also observed in earlier rectangular wing analyses<sup>5</sup> and is a direct effect of shock wave location. This result further demonstrates the importance of accounting for the presence of a shock wave and its location in designing an effective control law.

## References

- <sup>1</sup>Noll, T. E. and Huttzell, L. J., "Wing Store Active Flutter Suppression—Correction of Analyses and Wind-Tunnel Data," *Journal of Aircraft*, Vol. 16, July 1979, pp. 491-497.
- <sup>2</sup>Ballhaus, W., Goorjian, P., and Yoshihara, H., "Unsteady Force and Moment Alleviation in Transonic Flow," AGARD Conference Proceeding No. 227, May 1981.
- <sup>3</sup>Guruswamy, P. and Goorjian, P. M., "Efficient Algorithm for Unsteady Transonic Aerodynamics of Low-Aspect Ratio Wings," *Journal of Aircraft*, Vol. 22, March 1985, pp. 193-199.
- <sup>4</sup>Borland, C. J. and Rizzetta, D. P., "Nonlinear Transonic Flutter Analysis About Airfoils," *AIAA Journal*, Vol. 20, Nov. 1982, pp. 1606-1605.
- <sup>5</sup>Guruswamy, P., "An Integrated Approach for Active and Direct Coupling of Structures and Fluids," to appear in the *AIAA Journal*.
- <sup>6</sup>Persoon, A. J., Roos, R., Schippers, P., "Transonic and Low Supersonic Wind Tunnel Tests on a Wing with Inboard Control Surface," Air Force Flight Dynamics Lab., TR-80-3146, Dec. 1980.

## Effects of Contamination on Riblet Performance

Barry S. Lazos\*

NASA Langley Research Center  
Hampton, Virginia

## Introduction

THE parametric studies by Walsh and Lindemann and Wilkinson and Lazos,<sup>2</sup> among others, of various riblet geometries established riblets as an effective means for turbulent viscous drag reduction. These favorable experimental results have created an interest in the use of riblets for various applications (e.g., Refs. 3-6). Since many applications would expose the riblet surface to environments that could result in riblet surface contamination, a brief study of the effect of surface contaminants on riblet drag reduction has been conducted.

For riblet flight applications, contamination modes of particular interest include 1) atmospheric particulate matter that could collect on or between the ribs, and 2) contamination from liquids, such as oil and other miscellaneous condensates, that would concentrate in the riblet valleys but, in general, not extend above the riblet peaks. In the present study, thin-element plastic film riblets (provided by the 3M Corporation) were used that had been shown previously to behave similarly to v-groove riblets. Two different methods of contamination were used in an effort to simulate the two contamination modes of interest.

## Test Facility and Model Construction

The experiments were conducted in the closed-return,  $7 \times 11$ -in. (178 high  $\times$  279 wide  $\times$  914-mm long) low-speed wind tunnel at the NASA Langley Research Center over a velocity

Received June 4, 1988; revision received Sept. 25, 1988. Copyright © 1989 American Institute of Aeronautics and Astronautics, Inc. No copyright is asserted in the United States under Title 17, U.S. Code. The U.S. Government has a royalty-free license to exercise all rights under the copyright claimed herein for Governmental purposes. All other rights are reserved by the copyright owner.

range of 8–30 m/s ( $1000 < Re_\theta < 4000$ ) under nominally atmospheric conditions at nearly zero streamwise pressure gradient (the same facility used in previous riblet research.<sup>1,2,7</sup>) A portion of the tunnel test-section floor measuring 914 mm  $\times$  279 mm was used as the test bed. The turbulent boundary layer was tripped by a 1.5-mm-diam two-dimensional rod attached to the wall 254 mm upstream of the leading edge of the model. Drag data were acquired with a drag balance that consisted of a linear air-bearing and a piezoresistive force sensor. Models were mounted with small clearance gaps of approximately 0.45 mm at their leading and trailing edges and along their sides. Flow through the gaps was minimized by continuously monitoring and zeroing the difference between the test-section static pressure and the pressure in a surrounding control enclosure. Numerous flat-plate runs were made with each model to establish data repeatability. Drag measurements could be repeated to within 1%.

Riblet models were constructed by bonding plastic riblet film with an adhesive backing to a 914  $\times$  305-mm aluminum flat plate. Two riblet sizes, each with a different type of contaminant, were used for these tests. Both models were previously tested by Wilkinson and Lazos<sup>2</sup> to determine their drag-reducing effectiveness. Each model yielded different maximum levels of drag reduction due to different geometric dimensions. The performance differences in the models were not a concern, since for the present study the possible deleterious effects of contamination on a given riblet surface were of interest.

### “Contaminated” Riblet Models

The first model tested (Model 006006) had a riblet height and spacing of 0.152 mm. The contaminant was small bits of modeling clay pressed into the riblet channels used to simulate oil drops or condensates that would fill the riblet valleys and not extend above the riblet peaks. The clay was applied in rows of equally spaced spots along the span, with 11 spots per row. Each spot covered an average area of approximately 50 mm<sup>2</sup>. Figure 1 is an enhanced digitization of an actual cross-section photomicrograph of a representative portion of this contaminated model. It shows that the contaminant was in the riblet channels only and did not extend above the riblet peaks.

Three different levels of contamination were tested with the clay contaminant. Each level was determined by the amount of projected riblet surface area obstructed by the clay contaminant. The first level of contamination consisted of two rows of clay, one 19 mm from the leading edge and the other an

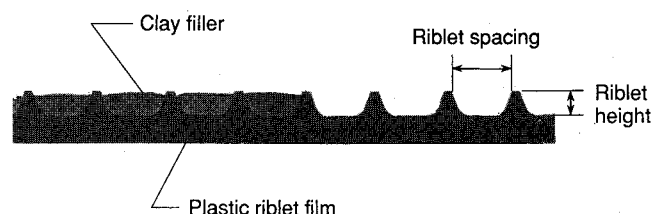


Fig. 1 Riblet Model 006006 with clay contaminant.

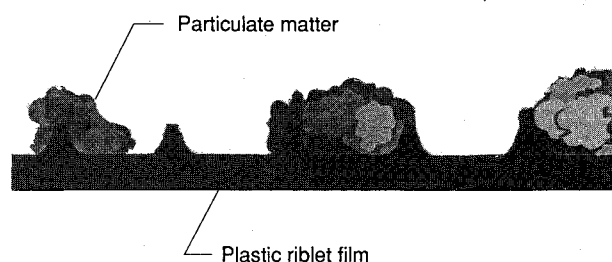


Fig. 2 Riblet Model 006012 with particulate contaminant.

equal distance from the trailing edge. The obstructed surface area (OSA) for this level was approximately 0.43%. The second and third levels consisted of five and nine evenly spaced rows of clay, respectively. The respective OSA's for these levels were approximately 1.08 and 1.95%.

The second model tested (Model 006012) had a riblet height and spacing of 0.152 and 0.305 mm, respectively. The contaminant used on this model was granulated eraser material (drawing cleaning powder). This particulate was chosen to give a relative size range (particle height/riblet height) that approximated the relative size range expected with atmospheric particles that might adhere to flight riblets, and the particles had irregular shapes as atmospheric particles would be expected to have. Because of surface shear forces during testing a large number of the particles did not remain on the riblet surface, but were carried off downstream. To prevent this, a thin film of nondrying adhesive was sprayed on the riblets. After the particles were applied, they were lightly pressed onto the surface. Tests were conducted to assure that the application of the adhesive alone did not affect riblet performance. The eraser materials particle height range was approximately 0.09 to 0.48 mm, with a mean height of approximately 0.22 mm, and a standard deviation of 0.11 mm. The height range was determined after the particles had been pressed onto the surface by microscopically viewing a representative section of similarly contaminated riblet material. Figure 2 is an enhanced digitization of an actual cross-section photomicrograph of a representative portion of this contaminated model. It shows that

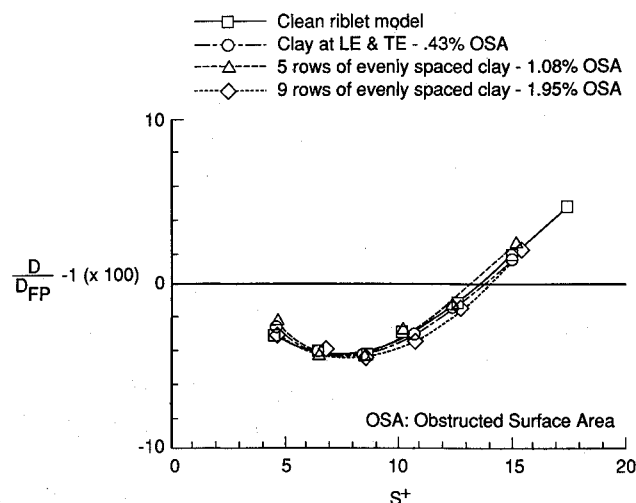


Fig. 3 Direct drag measurements for Model 006006 with clay contaminant.

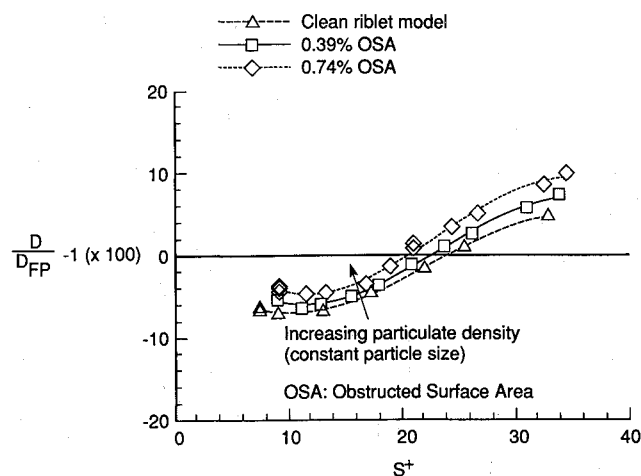


Fig. 4 Direct drag measurements for Model 006012 with particulate contaminant.

much of the particulate matter extended above the riblet peaks, while some completely filled the riblet valleys.

Two different levels of contamination were tested with the particulate contaminant. The OSA for each level was determined by statistical sampling. The first and second levels had OSA's of 0.39 and 0.74%, respectively.

### Results and Discussion

Figure 3 represents four sets of drag data for Model 006006 plotted with respect to riblet spacing in wall units  $s^+ = sU_\tau/\nu$  where  $s$  is the spacing,  $U_\tau$  the friction velocity, and  $\nu$  the kinematic viscosity. Three of the curves represent the three levels of clay contamination, while the fourth represents the clean riblet model. The figure shows that the contaminant did not significantly alter the maximum drag-reduction level.

These results suggest that the contaminants that completely fill the channels and do not extend above the riblet peaks effectively remove an active portion of the riblet surface area and have little effect on riblet performance as long as the contaminated area is small. However, it is expected that as the contaminated area is increased, the beneficial effects of riblets will be reduced as flat-plate conditions are approached. This was previously demonstrated by Walsh,<sup>7</sup> who showed a loss of riblet drag reduction when portions of the riblet surface were covered with transparent tape. The data indicated changes in drag reduction approximately proportional to the affected area.

Figure 4 shows the drag data for the two levels of particulate contamination used on Model 006012 along with the drag data for the clean model. Again, all curves are plotted with respect to  $s^+$ . The figure shows that as the OSA is increased, the performance level of the riblet model was reduced. The first and second levels of contamination yielded approximately a 1 and 2% loss in drag-reduction performance, respectively.

The majority of the particles used in these tests were in the relative size range 0.625–3.13 (particle height/riblet height). In a brief, unpublished study by the Boeing Commercial Airplane Company of particulate matter accumulation on flight application sized v-groove riblet panels, accumulated particles were found to be in the relative size range 0.098–1.18. Therefore, these tests represent a worst-case condition, where the particles are in the upper portion of and slightly beyond the relative size range of atmospheric particles found to accumulate on riblet material in the Boeing study. Though the size of accumulated atmospheric particles is expected to vary with geographical location (the Boeing study was conducted at a Seattle airport), the results from Boeing provided comparative information for the present riblet contamination tests. The tests indicate that the natural accumulation of atmospheric particles may result in a degradation in riblet performance.

Riblet surface static charge will play a complex role in atmospheric particle adhesion. Dipole and van der Waals forces intrinsic to the material can result in a surface charge that would tend to attract particles. Static charge caused by friction forces due to fluid motion over the riblet surface would also tend to attract particles. Simple surface chemistry modifications that would not alter the riblet shape may be possible and would minimize particle accumulation caused by such surface charges. This would be particularly effective in areas of the fuselage downstream of the nose and on the wings downstream of the leading edges where the streamlines do not stagnate.

Questions remain as to how local airflow will affect atmospheric particle accumulation on flight riblets. In a previously conducted laminar flow control (LFC) study concerned with the effects of insect debris on transition,<sup>8</sup> it was found that after flights of 2–3 h at heights of 40,000 ft or more, wings, legs, and other protuberances of the splattered insects had blown away. If atmospheric particles on flight application riblets are carried off by surface shear forces as the insect debris in the LFC study and the particulate matter in the present wind-tunnel study, particulate contamination may not be as serious as these tests might suggest.

It is important to note here that analogies cannot be made between particulate contamination effects on LFC<sup>8–10</sup> and particulate contamination effects on riblet performance. Any particulate large enough to cause transition would be detrimental to any LFC scheme, since the entire downstream flow region would be adversely affected. In the present case, the particles have only a local effect on the flow, so that normal turbulent flow conditions and drag reduction are returned downstream of the disturbance.

The importance of riblet contamination is still not clearly understood. Much will depend on how fast particles accumulate, how easily they are removed, and how the drag of a riblet-covered surface will increase with time as compared to a smooth surface exposed to the same contaminants. Further tests are still required under actual application conditions to understand more fully the importance of riblet contamination.

### Conclusions

Based on the results of this study, the following conclusions can be made:

- 1) Contaminants similar to those used in this study, such as oil drops and miscellaneous condensates, which concentrate in the riblet valleys and do not extend above the riblet peaks, appear to have no significant effect on riblet drag-reduction performance as long as the contaminated area is small. Riblet performance is expected to diminish to flat-plate values, though, as contaminated area approaches 100%.
- 2) Atmospheric particulate, having a relative size range that overlaps the relative size range used in this study, which attaches to the riblet surface, may degrade riblet performance. Simple surface chemistry modifications may be possible that would minimize this problem, particularly in regions on the fuselage, downstream of the nose, and on the wings, downstream of the leading edges.

### Acknowledgments

The author would like to thank Doug McLean of the Boeing Commercial Airplane Company for information gathered by Boeing. Special thanks also to Dr. Robert Baier at the State University of New York at Buffalo for information on possible techniques of riblet surface chemistry modifications.

### References

- <sup>1</sup>Walsh, M. J. and Lindemann, A. M., "Optimization and Application of Riblets for Turbulent Drag Reduction," AIAA Paper 84-0347, Jan. 1984.
- <sup>2</sup>Wilkinson, S. P. and Lazos, B. S., "Direct Drag and Hot-Wire Measurements on Thin-Element Riblet Arrays," IUTAM Symposium on Turbulence Management and Relaminarization, Bangalore, India, Jan. 1987.
- <sup>3</sup>Eilers, R. E., Koper, C. A., McLean, J. D., and Coder, D. W., "An Application of Riblets for Turbulent-Skin-Friction Reduction," *Proceedings of the 12th AIAA Symposium on the Aeronautics/Hydrodynamics of Sailing*, AIAA, New York, 1985, pp. 133–139.
- <sup>4</sup>"Mission Accomplished," NASA Tech Briefs, Vol. 11, No. 3, March 1987, pp. 82–83.
- <sup>5</sup>Van Valkenburg, P., "The Aerodynamics of the Bobsled," *Scientific America*, Feb. 1988, pp. t10–t14.
- <sup>6</sup>McLean, J. D., George-Falvy, D. N., and Sullivan, P. P., "Flight Test of Turbulent Skin-Friction Reduction by Riblets," *Turbulent Drag Reduction Conf. by Passive Means*, Royal Aeronautical Society, London, England, Sept. 1987, pp. 402–424.
- <sup>7</sup>Walsh, M. J., "Turbulent Boundary-Layer Drag Reduction Using Riblets," AIAA Paper 82-0169, Jan. 1982.
- <sup>8</sup>Lachmann, G. V., "Aspects of Insect Contamination in Relation to Laminar Flow Aircraft," Aeronautical Research Council, CP-484, 1960.
- <sup>9</sup>Peterson, J. B. and Fisher, D. F., "Flight Investigation of Insect Contamination and Its Alleviation," NASA CP-2036, 1978, pp. 357–373.
- <sup>10</sup>Coleman, W. S., "The Characteristics of Roughness from Insects as Observed for Two-Dimensional, Incompressible Flow Past Airfoils," *Journal of Aerospace and Science*, Vol. 26, 1959, pp. 264–280.